Biomacromolecules

ACS AUTHORCHOICE

pubs.acs.org/Biomac Article

Poly(alkanoyl isosorbide methacrylate)s: From Amorphous to Semicrystalline and Liquid Crystalline Biobased Materials

Siim Laanesoo, Olivier Bonjour, Jaan Parve, Omar Parve, Livia Matt, Lauri Vares,* and Patric Jannasch*

Cite This: *Biomacromolecules* 2021, 22, 640−648

Read Online

ACCESS | Metrics & More | Article Recommendations | Supporting Information

ABSTRACT: We have prepared a series of 12 D-isosorbide-2-alkanoate-5-methacrylate monomers as single regioisomers with different pendant linear C2−C20 alkanoyl chains using biocatalytic and chemical acylations. By conventional radical polymerization, these monomers provided high-molecular-weight biobased poly(alkanoyl isosorbide methacrylate)s (PAIMAs). Samples with C2−C12 alkanoyl chains were amorphous with glass transition temperatures from 107 to 54 °C, while C14−C20 chains provided semicrystalline materials with melting points up to 59 °C. Moreover, PAIMAs with C13−C20 chains formed liquid crystalline mesophases with transition temperatures up to 93 °C. The mesophases were studied using polarized optical microscopy, and rheology showed stepwise changes of the viscosity at the transition temperature. Unexpectedly, a PAIMA prepared from a regioisomeric monomer (C18) showed semicrystallinity but not liquid crystallinity. Consequently, the properties of the PAIMAs were readily tunable by controlling the phase structure and transitions through the alkanoyl chain length and the regiochemistry to form fully amorphous, semicrystalline, or semi/liquid crystalline materials.

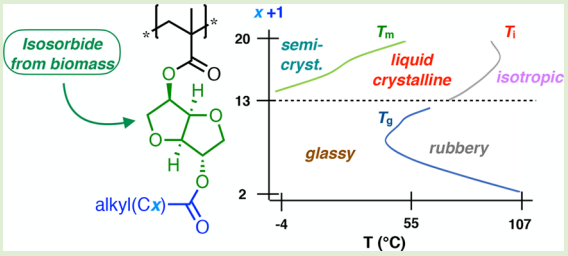

INTRODUCTION

Consumption of finite fossil resources combined with growing environmental concerns is a strong driving force to phase out oil-based chemical processes and utilize renewable biomass as a source for chemicals and plastics.[1] However, it is a great challenge to develop economically viable routes to bioderived plastics that have good processability and fulfill all of the material property requirements for various applications.[2] Biobased polymers with a high glass transition temperature (T_g) have been especially challenging to achieve.[3] In this context, rigid bicyclic isosorbide produced from D-glucose on an industrial scale[4] has been identified as one of the platform building blocks with the potential to replace fossil-based counterparts in high-T_g plastics.[5] Isosorbide is a nontoxic, chiral, V-shaped diol, bearing two sterically different secondary hydroxyl groups (with *exo* and *endo* configurations, respectively) and two *cis*-connected tetrahydrofuran rings.[6]

The use of isosorbide has been extensively investigated for the synthesis of step-growth polymers such as polyesters, polycarbonates, polyamides, and polyurethanes, some of which are commercially available.[7,8] Furthermore, diepoxy,[9,10] divinyl,[11,12] and di(meth)acrylate[13−15] monomers of isosorbide have been prepared and their polymerization investigated. In most cases, the *exo* and *endo* hydroxyl groups have not been differentiated and the isosorbide unit has been fully incorporated into the polymer backbone. Far less studied are selective functionalizations where the polymerizable functionality has been attached exclusively on either the *exo* or the *endo* hydroxyl group. In such an arrangement, the isosorbide unit is not built into the polymer backbone but instead forms pendant side groups. Thus, the residual free hydroxyl group on the isosorbide unit enables the attachment of various substituents to control properties (e.g., the T_g) or to introduce different reactive functionalities, e.g., for use in subsequent cross-linking reactions.

Regioselective synthesis of isosorbide monoesters has been a field of research for decades, mainly because there has been a lack of a universal method for regioselective catalytic acylation of the isosorbide hydroxyl groups. Both chemocatalytic and biocatalytic methods have been investigated. Apart from some early chemical methods based on heavy metal salts,[16] a 4.2:1 *endo* selective $Sc(OTf)_3$ catalyzed process has been reported by Hillmyer et al.[17] In addition, Aldabbagh and co-workers have developed MeMgCl-mediated conditions to selectively prepare both *exo* and *endo* acetates.[18] However, this method requires equimolar amounts of MeMgCl.[18] Biocatalytic pathways have been studied more intensively.[19−23] For example, a solvent-free Lipozyme-catalyzed procedure has been shown to provide products with high regioselectivity in the case of acyl groups with longer carbon chains but afforded poor results for shorter

Received: October 13, 2020
Revised: November 27, 2020
Published: December 12, 2020

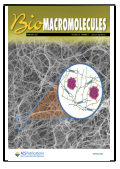

https://dx.doi.org/10.1021/acs.biomac.0c01474
Biomacromolecules 2021, 22, 640−648

ones.[19] In general, both 2-acylates[22] and 5-acylates[21,24] have been prepared with better results obtained for the latter compound. We have recently reported on a highly regioselective lipase-catalyzed method for the monomethacrylation of isosorbide using either vinyl methacrylate or methacrylic anhydride as the methacryl donor.[24] This readily upscalable approach enables the preparation of both isosorbide-5-methacrylate (5-**IMA**) and isosorbide-2-methacrylate (2-**IMA**) with essentially complete regioselectivity (>99:1 for both isomers).

Isosorbide monomethacrylates have been polymerized by both conventional free-radical,[17,24] reversible addition-fragmentation chain transfer (RAFT)[17] and single-electron transfer-living polymerization techniques.[25] Still, the number of studies concerning the effect of different isosorbide substitutions on polymer properties is very limited. Unsubstituted monomer 5-**IMA** provides a polymethacrylate with T_g = 167 °C, which is soluble in dimethyl sulfoxide (DMSO) but not in other common solvents such as alcohols, water, chlorinated solvents, or tetrahydrofuran (THF).[24] Atactic polymers prepared from acetylated isosorbide methacrylate show T_g at approximately 127 °C and are also soluble in THF, acetonitrile (ACN), and $CHCl_3$. This hints that these polymers may potentially be considered as a biobased alternative to poly(methyl methacrylate) in some applications.

Data on the effects of monomer regiochemistry on polymer properties is very scarce, mostly due to the lack of straightforward and highly regioselective monomethacrylation methodologies. In the case of acetylated isosorbide polymethacrylates, the regiochemistry has no significant impact on the thermal properties of the polymers.[17,24] However, in the case of dodecanoate substitution, the effect is pronounced: the polymer with the pendant dodecanoate chain in the *exo* position shows crystallinity and a high melting point (T_m = 83 °C), whereas the polymer with the dodecanoate chain in the *endo* position is fully amorphous with T_g = 54 °C.[24] Differences in T_g values and solubility properties have also been reported in the case of regioisomeric poly(vinyl isosorbide triazole)s.[26] These findings imply that the properties of isosorbide polymethacrylates can be conveniently controlled over a wide range by the choice of the pendant substituent. Consequently, this class of materials may then be tuned for different applications, including engineering plastics, optical, and coating applications. This motivates detailed characterizations and studies of different structure−property relationships.

In the present work, we have prepared a range of isosorbide polymethacrylates as single regioisomers substituted with linear alkanoates of different lengths with the main goal to systematically study their phase behavior, thermomechanical and rheological properties, and processability. In addition, we also report on an efficient and upscalable biocatalytic method with which a series of isosorbide-5- and 2-methacrylic diester monomers bearing 12 different alkanoate substituents extending from acetate (C2) to eicosanoate (C20) was synthesized. The monomers were employed in conventional free-radical polymerizations, and the resulting poly(alkanoyl isosorbide methacrylate)s (PAIMAs) were characterized by thermogravimetry, calorimetry, rheology, dynamic mechanical analysis (DMA), and microscopy.

EXPERIMENTAL SECTION

Materials. Reagents and solvents were obtained from commercial sources and used as received. As a precaution, a small amount of a radical scavenger [hydroxyquinone (HQ) or *p*-methoxyphenol (HQMME)] was added to the methacrylate monomers after preparation and the monomers were stored in a refrigerator (2−6 °C). The isosorbide acylations were monitored by thin-layer chromatography (TLC, Xtra SIL G/UV_{254}), and the plates were visualized by staining with a phosphomolybdic acid solution. Silica gel 60 (0.040−0.063 mm, 230−400 mesh) was used for flash chromatography.

Structural Characterization. Monomer and polymer structures were characterized using a Bruker 400 MHz NMR spectrometer with samples dissolved in chloroform-*d*. The ^{1}H and ^{13}C NMR spectra were measured at 400.1 and 100.6 MHz, respectively. The chemical shifts are given in ppm, and residual solvent signals were used for calibration (for ^{1}H, $CDCl_3$: δ = 7.26 ppm, for ^{13}C, $CDCl_3$: δ = 77.0 ppm). The conversions in the polymerization step were measured by comparing the broad non-overlapping polymer signal at 4.90−5.10 or 4.70−4.90 ppm with the remaining double bond signal at approximately 6.15 ppm (*trans*-H) in the monomer. High-resolution mass spectrometry (HRMS) analyses of monomers were carried out on a Thermo Electron LTQ Orbitrap XL analyzer, and Fourier transform infrared (FTIR) analyses were performed on a Shimadzu IRAffinity-1 spectrometer. The molecular weights of the polymers were determined by size-exclusion chromatography (SEC) with THF as the solvent. A Shimadzu Prominence system equipped with three Shodex columns (KF-805, −804, and −802.5, coupled in series) and a refractive index detector (RID-20A) was used. Samples were run at 40 °C with an elution rate of 1 mL min^{-1}. Poly(ethylene oxide) standards (M_n = 3860, 12 600, 49 640, and 96 100 g mol^{-1}) were used for calibration, and the results were analyzed using Shimadzu LabSolution software.

Monomethacrylate Synthesis. The monomers **AIMA2**−**AIMA20** and *r*-**AIMA18** as single regioisomers were prepared from 5-**IMA** (*endo*/*exo* > 99:1) and 2-**IMA** (*exo*/*endo* > 99:1), respectively, via either biocatalytic (Novozym 435/vinyl alkylate) or chemical (acyl chloride/Et_3N) acylation in up to 36 g scale. The monomers were purified by a simple extraction/filtration sequence (in case of optimized large-scale synthesis of **AIMA2** and **AIMA4**) or by flash chromatography. Detailed experimental procedures and analytical data for all monomers are presented in the SI.

Alkanoyl Isosorbide Methacrylate Polymerization. After removal of the inhibitor (described in the SI), the diester monomer and AIBN (0.5 mol %) were dissolved in EtOAc (0.1 g mL^{-1}) and transferred to the reaction flask. The solution was purged with argon gas for 30−60 min, whereafter the reaction flask was sealed and placed in a preheated oven at 63 °C for 24 h. After being allowed to cool, the crude polymer was precipitated in methanol (product concentration 2 g L^{-1}). The solids were filtered, washed with an additional amount of methanol, and dried under reduced pressure to obtain the target polymer.

Thermal Analysis. Thermogravimetric analysis (TGA) was performed on a TA Instruments TGA Q500. Samples of 1−8 mg were heated to 600 °C at a rate of 10 °C min^{-1} under nitrogen flux (60 mL min^{-1}). The thermal decomposition temperature ($T_{d,95}$) was determined at a 5% loss of the initial weight. Differential scanning calorimetry (DSC) measurements were performed on TA Instruments DSC Q2000. Samples of 1−10 mg were first heated to 120 or 200 °C (depending on their respective thermal decomposition temperatures) at a rate of 10 °C min^{-1}. They were maintained at this temperature for 2 min, before cooling to −50 °C, and were then maintained isothermally for 2 min, before being heated back to the starting temperature at the same heating rate.

Dynamic Mechanical Measurements. Dynamic mechanical analysis (DMA) was carried out on a TA Instruments DMA Q800. Rectangular bars (35 × 5 × 1 mm) of samples **P2** and **P3** were hot-pressed in a steel mold placed between two Teflon plates using a hydraulic press (Specac, GS15011) at 150 °C for 2 min. The samples

https://dx.doi.org/10.1021/acs.biomac.0c01474
Biomacromolecules 2021, 22, 640−648

Scheme 1. Regioselective Synthesis of the Alkanoyl Isosorbide Monomethacrylates[a]

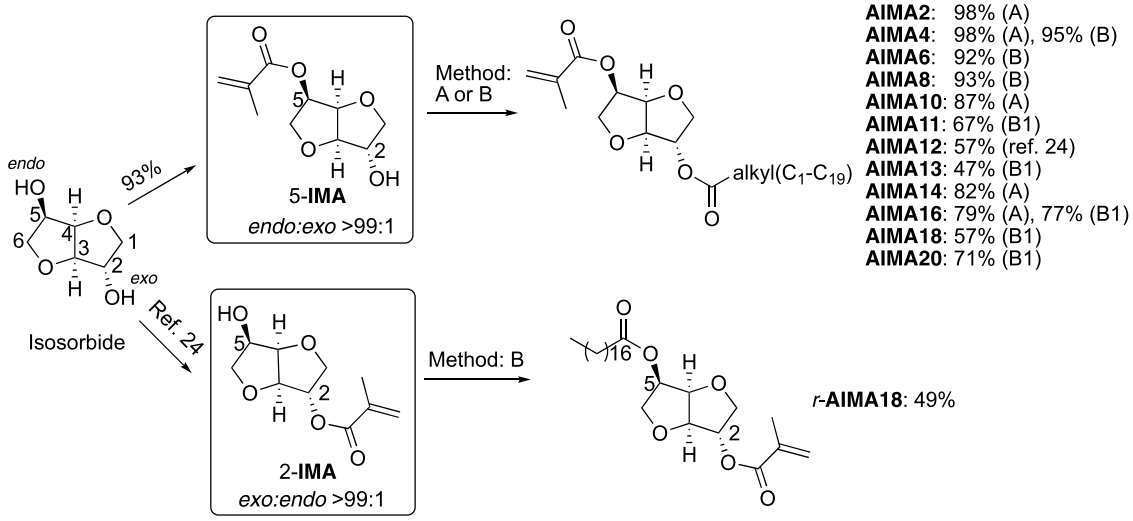

[a]Method **A**: corresponding vinyl alkylate, Novozym 435, and ACN/PE. Method **B**: corresponding acyl chloride, Et_3N, ACN, or CH_2Cl_2 (**B1**).

were then cooled to 100 °C for 5 min and finally to room temperature. Analysis of the samples was carried out at 1 Hz in the temperature range between 25 and 150 °C at a heating rate of 2 °C min^{-1}. The measurements were performed in the linear viscoelastic region at a strain of 0.01%. The T_g value was determined by the maximum peak value of the loss modulus (G'') in the glass transition region.

Melt Rheology. Dynamic rheology measurements were performed with a TA Instruments Advanced Rheometer AR2000 ETC. The experiments were carried out using parallel plates (Ø = 25 mm). Disks of samples **PAIMA16**, **PAIMA18**, and **PAIMA20** (Ø = 25 mm, t = 1 mm) were hot-pressed as described above. A time sweep was carried out on sample **PAIMA18** for 40 min at 100 °C, 1 Hz, and 1% strain, which was within the linear viscoelastic region. Moreover, a temperature sweep was performed on **PAIMA16**, **PAIMA18**, and **PAIMA20** with a strain of 0.01% at 1 Hz. These samples were first cooled from 120 to 75 °C at a rate of 2 °C min^{-1} and then heated to 120 °C before being cooled to 75 °C at the same rate.

Light Microscopy. The phase behavior and structure of **PAIMA20** were observed using an Olympus BX50 microscope under cross-polarized light. The sample was heated and cooled using a Linkam THMS 600 hot stage mounted on the microscope and controlled by a Linkam TMS 93 temperature controller. **PAIMA20** was first melted at 120 °C on a 16 mm clear glass stage plate and then covered with another glass plate. The sample was then slowly cooled to room temperature to allow for crystallization. Photographs were taken using a Lumenera INFINITY 2, 2.0 USB Microscope Camera and Lumenera's Infinity Analyse software.

RESULTS AND DISCUSSION

Synthesis of Isosorbide Methacrylic Diester Monomers. An important issue to consider when designing a synthesis is the required scale. At the proof-of-concept level, monomers in quantities up to ca. 2−5 g are commonly needed, and at this scale, there are fewer restrictions regarding processing (including purification) and economy. However, for application tests, where usually preparative synthesis in >30 g scale is required, the development of a readily upscalable procedure normally becomes necessary. For example, the properties of potential byproducts and the choice of an efficient product purification method become crucial if highly reactive monomers need to be produced with high purity on such a scale.

In general, the 5-OH group (*endo*) in isosorbide is sterically shielded but is on the other hand a stronger nucleophile than the 2-OH group (*exo*) due to intramolecular hydrogen bonding. Therefore, the chemical acylation of isosorbide generally favors the sterically less accessible, but chemically more reactive, 5-OH group. Somewhat unexpectedly, such a selectivity toward the 5-OH group has also been observed for most (but not all) of the lipases used to catalyze the regioselective acylation of isosorbide. In the current work, a two-step lipase-catalyzed process was used for the regioselective synthesis of several diester monomers. The first step was methacrylation of the 5-OH group using *Rhizomucor miehei*(RM) lipase as a catalyst. RM lipase should be immobilized on resin; the variant immobilized on immobead was found to be inactive in this application. The procedure applied here is an improved version of our previously reported method[24] and provides 5-**IMA** in 93% yield (Scheme 1, previously 87%) using a straightforward chromatography-free workup (purity and regioselectivity >99%; see the SI for the detailed procedure).

For the second acylation, both a biocatalytic and a conventional chemical procedure (acyl chloride/Et_3N) were evaluated. In the biocatalytic reaction (method A, Scheme 1), we utilized *Candida antarctica* lipase B, which is less selective in this system. Consequently, it was able to catalyze the acylation of the 2-OH group in the 5-monoester intermediate with a variety of acyl groups, albeit at a somewhat elevated temperature (45 °C). These syntheses provided highly homogeneous diesters in good to excellent yields (79−98%, Scheme 1). The excess acyl donors (i.e., vinyl esters) with short acyl hydrocarbon chains (C2, C4) were smoothly separated by distillation at reduced pressure on a rotary evaporator after the reaction was completed. The diester products were purified by decolorization using activated charcoal in ethanol. Such a straightforward separation methodology is particularly important when upscaling the synthesis.

The alkanoyl isosorbide methacrylate monomers in this study are denoted as **AIMA*x***, where x indicates the number of carbon atoms of the pendant alkanoate substituent. For **AIMA2** and **AIMA4**, we optimized acetylation and butyr-

https://dx.doi.org/10.1021/acs.biomac.0c01474
Biomacromolecules 2021, 22, 640−648

ylation, respectively, on a ∼30 g scale and obtained the target diesters using a chromatography-free process in >98% yield (purity and regioselectivity >99%). For **AIMA6**, **AIMA8**, **AIMA13**, **AIMA18**, and **AIMA20**, a conventional acyl chloride/Et_3N procedure was used (method B and B1, Scheme 1). The yields were generally somewhat lower compared to the biocatalytic method. However, no particular optimization was attempted for these monomers, and we focused instead on monomer purification. In general, the choice of a particular synthetic method depends not only on the goal and the scale but also on the availability of a specific acyl donor.

The regioisomeric 2-**IMA** was prepared according to our previous report,[24] and the subsequent reaction with stearoyl chloride provided *r*-**AIMA18** in 49% yield. Monomers with short and medium-size alkanoyl substituents (**AIMA2**−**AIMA13**) were viscous liquids, whereas longer alkanoyl-substituted monomers were white crystalline compounds (**AIMA14**−**AIMA20**, *r*-**AIMA18**). The solubility of the monomers was also affected by the length of the alkanoyl chain, and the physical state in the series of monomers changed noticeably between **AIMA13** and **AIMA14**. Monomers with longer alkanoyl chains (**AIMA14** and beyond) were soluble in ethereal solvents (THF, diethyl ether) but were insoluble in highly polar DMSO. Monomer **AIMA2** is an exception since it was also soluble in ethereal solvents. In general, all of the studied monomers were readily soluble in EtOAc, toluene, ACN, $CHCl_3$, and MeOH, and 5-**IMA** was also soluble in water (for detailed solubility data, see Table S1).

Polymerization of Alkanoyl Isosorbide Methacrylate Monomers. All of the monomers were polymerized in EtOAc solutions at 63 °C for 24 h using conventional free-radical polymerization initiated by AIBN (0.5 mol %), as seen in Scheme 2. Only in the case of **AIMA20**, a few droplets of CH_2Cl_2 were added to the reaction mixture to avoid cloudiness as this monomer had limited solubility in EtOAc. Alternatively, toluene was successfully used as a polymerization medium for **AIMA20**. The resulting series of poly(alkanoyl isosorbide methacrylate)s were denoted as **PAIMA*x***. MeOH readily dissolved all of the monomers and was chosen for the precipitation of the polymers from the reaction mixtures. In the case of **PAIMA20**, the isolated polymer was washed multiple times with MeOH as the residual **AIMA20** monomer dissolved slowly in MeOH. All of the isolated polymers were white solids and their structures were confirmed by ^{1}H NMR spectroscopy. The number average molecular weight (M_n) and polydispersity ($Đ$) were determined by SEC using poly(ethylene oxide) standards (Table 1). The monomer conversions ranged from 56 to 96% (Table 1), and M_n varied between 32 and 81 kg mol^{-1}. In addition to the homopolymers, a 1:1 mixture of **AIMA18** and *r*-**AIMA18** was also successfully copolymerized [**P(AIMA18-*co*-*r*-AIMA18)**, entry 14]. The solubility of the polymers was investigated in a wide range of solvents with different solubility parameters (δ) and hydrogen-bonding capacity (Table S2).[27] All polymers with alkanoyl substituents were soluble in EtOAc, $CHCl_3$, and THF. Toluene dissolved all polymers except **PAIMA2**. Solvents with a strong hydrogen-bonding capacity (H_2O, MeOH, *n*-BuOH) did not dissolve any of the polymers. The polar aprotic DMSO dissolved polymers with short alkanoyl chains (**PAIMA2** and **PAIMA4**), but polymers with longer alkanoyl chains remained insoluble. Acetonitrile, having a δ value similar to that of DMSO, dissolved **PAIMA2**, **PAIMA4**, and **PAIMA6**. The *r*-**PAIMA18** and **P(AIMA18-*co*-*r*-AIMA18)** copolymers had a similar solubility profile as **PAIMA18** (Table S2).

Scheme 2. Polymerization of the Alkanoyl Isosorbide Methacrylates by Conventional Radical Polymerization

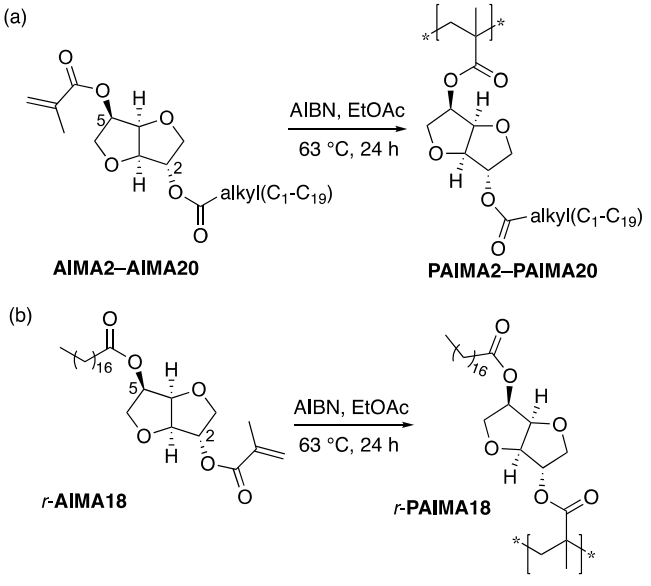

Thermal Stability. The polymers were analyzed by thermogravimetric analysis (TGA) to study the thermal decomposition of the polymers under a N_2 atmosphere. The TGA traces in Figure 1a show that the decomposition temperature ($T_{d,95}$) varied between 190 and 259 °C (see Table 1), and the derivatives of the TGA traces in Figure 1b indicate two distinguishable steps. As reported by Matt et al., the first step most likely corresponds to the decomposition of the alkanoyl chains, and the second step to the degradation of the isosorbide units, followed by a gradual decomposition of the polymer backbone.[24] The plot of $T_{d,95}$ versus the number of carbon atoms in the pendant alkanoyl chain shows an initial decrease from 238 °C for the non-alkanoylated **PAIMA0**[24] to 190 and 188 °C for **PAIMA4** and **PAIMA6**, respectively. After this decline, $T_{d,95}$ increases almost linearly with the alkanoyl chain length up to 259 °C for **PAIMA20**. This variation may possibly be explained by the high T_g (high melt viscosity) of the material without alkanoyl chains (x = 0), resulting in high $T_{d,95}$ values. With increasing chain length (x = 2 and 4), T_g decreased, and consequently, $T_{d,95}$ decreased to 190 °C. As the chain length increased further (x = 6−20), the gradual increase in $T_{d,95}$ may be explained by the dilution of the heat-sensitive isosorbide in the samples as the alkanoyl chain length and content increased (Figure 2).

Fully Amorphous Materials. Differential scanning calorimetry (DSC) showed a large variation in phase behavior depending on the length of the pendant alkanoyl chain. **PAIMA0**, with unsubstituted 2-OH, is a fully amorphous material with a high T_g (167 °C) because of the hydrogen bonding of the hydroxyl groups.[24] As seen in Figure 3a, the DSC traces of polymers substituted with short alkanoyl chain lengths indicated only glass transitions and were thus also fully amorphous materials. As expected, the T_g decreased with increasing chain length because of the increasing internal plasticization by the flexible alkanoyl chain. Thus, the T_g decreased from 107 °C for **PAIMA2** to 80 °C for **PAIMA4**, whereafter the value seemingly stabilized between 57 and 52

https://dx.doi.org/10.1021/acs.biomac.0c01474
Biomacromolecules 2021, 22, 640−648

Table 1. Polymerization and Thermal Data of the PAIMA*x* Samples

entry	sample	monomer conv. (%)[b]	M_n (kg mol^{-1})[c]	$Đ$[c]	$T_{d,95}$ (°C)[d]	T_g (°C)[e]	T_m (°C)[e]	T_c (°C)[e]	ΔH_m (J g^{-1})[e]	T_i (°C)[e,f]	T_a (°C)[e,g]	ΔH_i (J g^{-1})[e]
1	PAIMA0[a]	96	n.a	n.a	238	167						
2	PAIMA2	85	32	2.97	208	107						
3	PAIMA4	84	60	1.78	190	80						
4	PAIMA6	63	56	2.11	188	57						
5	PAIMA8	76	38	2.16	199	46						
6	PAIMA10	56	47	2.06	201	52						
7	PAIMA11	79	56	2.27	209	56						
8	PAIMA12[a]	87	43	2.70	226	66						
9	PAIMA13	81	32	2.23	228					75	65	2.2
10	PAIMA14	82	61	2.23	233		−4	−10	5.5	82	73	2.0
11	PAIMA16	82	58	2.11	231	76	19	10	20	92	79	2.7
12	PAIMA18	75	62	2.63	254	79	32	26	16	97	90	1.5
13	*r*-PAIMA18	58	49	2.06	251		30	23	33			
14	P(AIMA18-*co*-*r*-AIMA18)	75	81	2.14	247		41	35	41	69	59	0.5
15	PAIMA20	81	46	2.57	259	74	55	46	53	94	88	2.1

[a]Data taken from ref 24. [b]Determined by ^{1}H NMR spectroscopy. [c]Measured by SEC in THF using poly(ethylene oxide) standards. [d]Measured by TGA at 5% weight loss under N_2. [e]Determined by DSC. [f]Isotropization temperature measured during heating. [g]Anisotropization temperature measured during cooling.

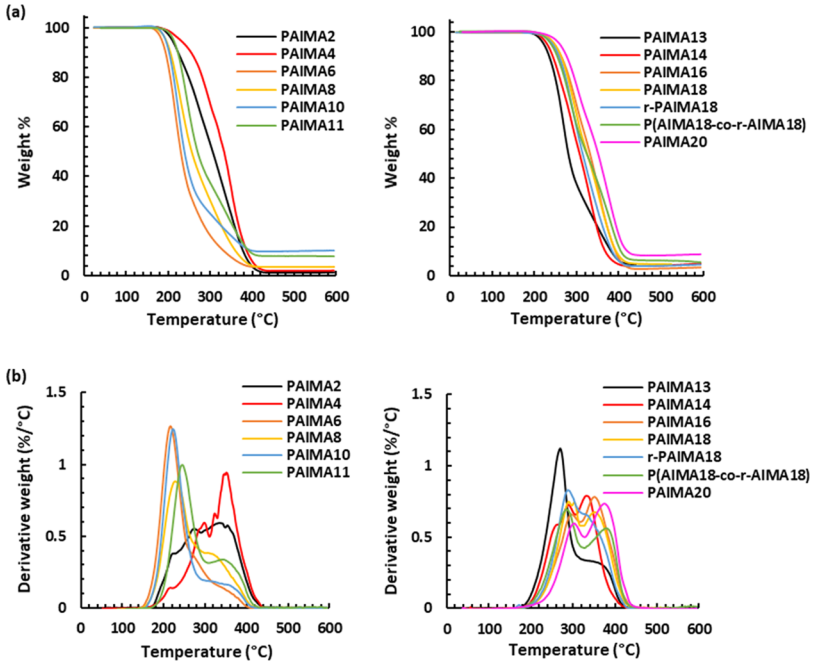

Figure 1. TGA (a) and corresponding differential TGA (b) profiles of the **PAIMA*x*** series recorded under a N_2 atmosphere at 10 °C min^{-1}.

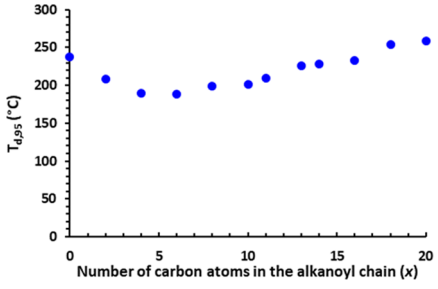

Figure 2. Variation of $T_{d,95}$ with the number of carbon atoms in the alkanoyl chain in the **PAIMA*x*** series with x = 0−20.

°C for **PAIMA6**, **-8**, **-10**, **-11**, and **-12** (notably, the T_g of **PAIMA8** is 46 °C but may be explained by the quite low M_n of this sample). The T_g values of both **PAIMA0** and **PAIMA2** reached above 100 °C, which makes these materials interesting for high-temperature applications such as "hot-fill" applications in packaging.

Dynamic mechanical analysis (DMA) was carried out on hot-pressed samples of **PAIMA2** and **PAIMA4** to study the mechanical stiffness and glass transitions of these materials. Figure 4 shows the storage (E') and loss (E'') moduli as a function of temperature in the linear viscoelastic region. As expected, the materials had a high mechanical stiffness at the glassy plateau, which then decreased as the glass transition was reached. Hence, for **PAIMA2** and **PAIMA4**, the storage

https://dx.doi.org/10.1021/acs.biomac.0c01474
Biomacromolecules 2021, 22, 640−648

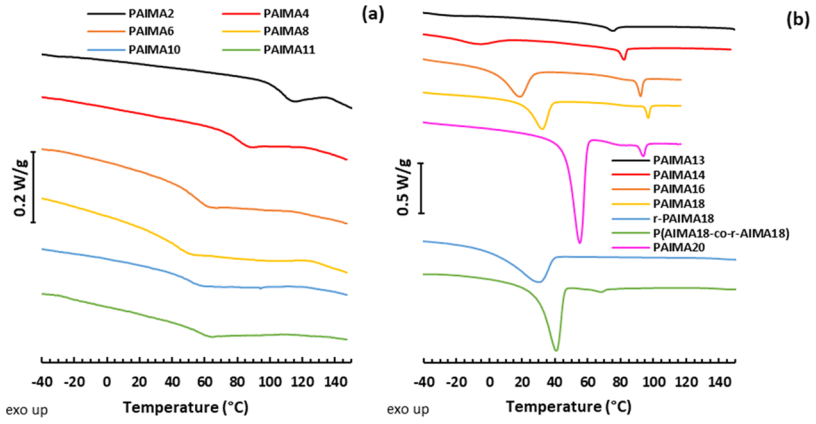

Figure 3. DSC heating traces of the polymers in the **PAIMA*x*** series: (a) x = 2−11 and (b) x = 13−20, also including the samples *r*-**PAIMA18** and **P(AIMA18-*co*-*r*-AIMA18)**.

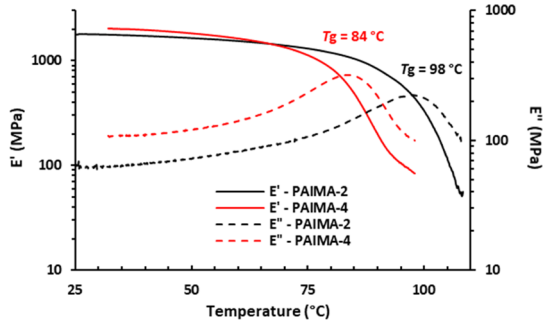

Figure 4. Storage (E') and loss (E'') moduli of **PAIMA2** and **PAIMA4** measured by DMA at 2 °C min^{-1} in the linear viscoelastic region (0.01% strain, 1 Hz).

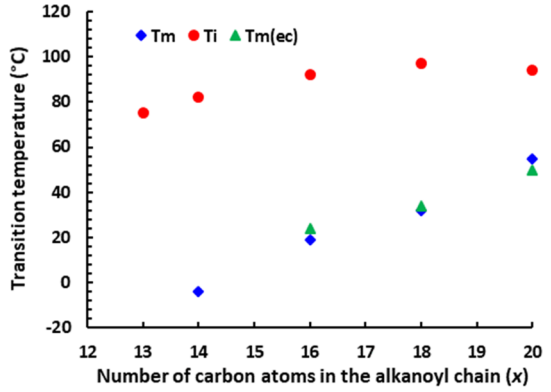

Figure 5. Variation of the crystalline melting point (T_m) and the isotropization temperature (T_i) in the **PAIMA*x*** series with x = 13−20 compared with the crystalline melting point of ethyl carboxylates [T_m(ec)] with x = 16−20.

modulus only went below 1 GPa at temperatures above 86 and 77 °C, respectively. The T_g values (taken at the local maximum of the loss modulus) were found at 98 and 84 °C for **PAIMA2** and **PAIMA4**, respectively. These values may be compared with 107 and 80 °C, respectively, measured by DSC.

Semicrystalline and Liquid Crystalline Materials. As the length of the pendant alkanoyl chain was increased to above x = 13, the polymers in the **PAIMA*x*** series became semicrystalline (Table 1). Consequently, **PAIMA14** showed a first-order transition attributed to crystalline melting (Figure 5). The melting point (T_m) then increased with alkanoyl chain length from −4 for **PAIMA14** to 55 °C for **PAIMA20** (Figure 5). Concurrently, the melt enthalpy (ΔH_m) increased from 5.5 to 53 J g^{-1} (Table 1). Glass transitions were detected at 74−79 °C for **PAIMA16**, **−18**, and **−20**, i.e., at significantly higher values than for PAIMA6, **−8**, **−10**, **−11**, and **−12** (Table 1). This increase of T_g with the alkanoyl chain length may indicate that the polymethacrylate backbone is not plasticized by the flexible alkanoyl chains, which in turn suggests that these two components were phase-separated when x exceeded a certain number between 12 and 16.

The T_g and T_m values of the **PAIMA*x*** series may be compared to those of corresponding poly(n-alkyl methacrylate)s. For example, high-molecular-weight poly(octadecyl methacrylate) shows T_g and T_m values of −100[28] and 37.5 °C,[29] respectively. In addition, the T_m of the PAIMAs with the longest alkanoyl chains (x = 16−20) matched the values of corresponding ethyl carboxylates (Figure 5). Hence, the T_m values of the ethyl esters of hexadecanoic, octadecanoic, and eicosanoic acid are 24, 34, and 50 °C, respectively.[30−32]

Another first-order transition was observed by DSC well above T_m for samples with a pendant alkanoyl chain length above 12 carbon atoms (Figure 5). For **PAIMA14**, this transition occurred at an isotropization temperature of T_i = 82 °C during heating, i.e., 86 °C above T_m (−4 °C). The transition enthalpy (ΔH_i) varied between 1.5 and 2.7 J g^{-1}, well below that of ΔH_m, seemingly independent of the alkanoyl chain length. We interpreted this as an order-to-disorder transition that appeared in connection with the formation of a liquid crystalline mesophase after crystalline melting. The transition temperature seemed to increase with the alkanoyl chain length (small variations may be explained by differences in molecular weight) from T_i = 82 for **PAIMA14** to 97 and 94 °C for **PAIMA18** and **PAIMA20**, respectively (Figure 5). The corresponding anisotropization temperature (T_a) recorded during cooling was between 6 and 10 °C below T_i, revealing a reversible hysteresis behavior (Table 1).

To observe the phase transitions and further confirm the formation of a liquid crystalline mesophase, **PAIMA20** was studied during heating (10 °C min^{-1}) by optical microscopy under cross-polarized light. Typical micrographs of the optical textures at different temperature regimes are shown in Figure 6. First, the micrograph taken at 22.5 °C (i.e., below T_m) displays the typical spherulitic texture of a semicrystalline polymer (Figure 6a). In this case, the spherulites had an average diameter of ∼100 μm. Upon heating, the crystallites

https://dx.doi.org/10.1021/acs.biomac.0c01474
Biomacromolecules 2021, 22, 640−648

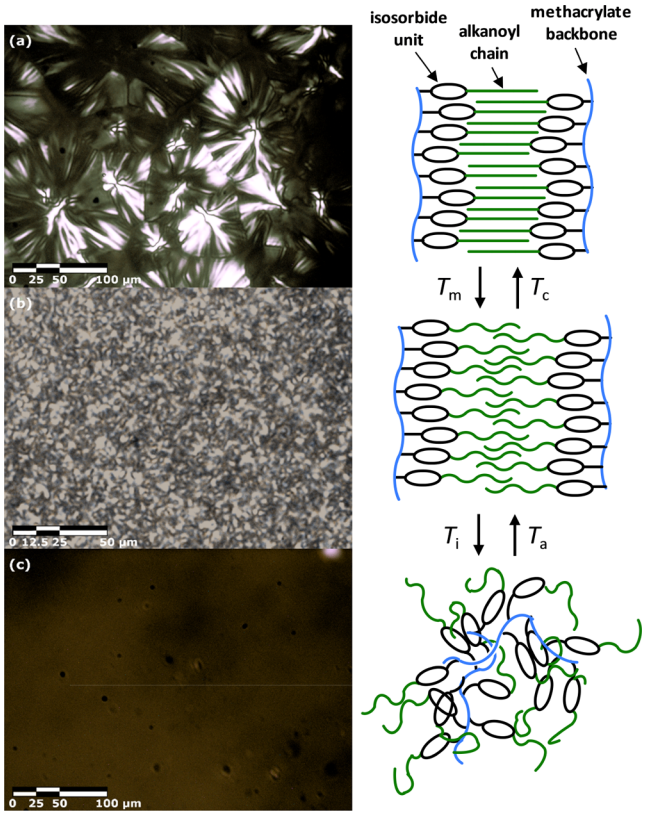

Figure 6. Cross-polarized optical micrographs of **PAIMA20** showing a semicrystalline spherulitic texture at 22.5 °C (a), a fine grainy texture indicating a liquid crystalline mesophase at 52.2 °C (b), and the absence of any texture at 113 °C to indicate a fully isotropic polymer melt (c). The illustration shows a simplified representation of the polymers and the different phase structures.

started to melt, and the spherulitic texture completely disappeared at around 50 °C. Instead, a fine granular texture started to appear, indicating the formation of a mesophase, most probably a nematic liquid crystalline phase (see Figure 6b). When the sample was further heated, this texture became finer and then gradually disappeared. No texture was observed above 95 °C, which indicated a fully isotropic polymer melt (Figure 6c). Consequently, all of the results and conclusions from the DSC study concerning the phase behavior of **PAIMA20** were corroborated by optical microscopy observations.

As far as we know, no mesophases have been reported for poly(*n*-alkyl methacrylate)s. Hence, the liquid crystallinity of the **PAIMA*x*** series was most probably induced by the stiff and stereoregular isosorbide units, which acted as mesogenic groups. He et al. have previously reported on the use of isosorbide as the core units of liquid crystalline materials.[33] Moreover, Zhang and co-workers have prepared and studied side-chain cholesteric liquid crystalline polymers containing aromatic mesogenic groups and isosorbide as a chiral center.[34] However, to the best of our knowledge, the present work demonstrates for the first time the use of isosorbide as a mesogenic group, giving rise to order−disorder transitions close to 100 °C. The polymers discussed up to this point were all based on 5-methacrylic 2-diester monomers. To study the influence of the isosorbide substitution, we prepared and studied *r*-**PAIMA18** (based on 2-methacrylic 5-diester monomer, Scheme 2). Both polymers with x = 18 showed semicrystallinity with T_m at approximately 30 °C (Table 1). However, whereas **PAIMA18** showed a clear transition at T_i = 97 °C, *r*-**PAIMA18** showed no such transition, indicating the absence of any mesophase (Figure 3). In addition, a copolymer was prepared from monomers **AIMA18** and *r*-**AIMA18** (Scheme 1) (50:50, mol/mol). This copolymer showed a crystalline melting point at 41 °C and a very small (ΔH_m = 0.5 J g^{-1}) endothermic order−disorder transition at 69 °C, well below that of **PAIMA18** (97 °C). Hence, the small mesophase detected for the copolymer may likely be exclusively formed by 5-methacrylic diester monomer residues. In conclusion, it seemed like **PAIMA*x*** samples based on 5-methacrylic diester monomers with sufficiently long alkanoyl chains (x > 12) form mesophases, while the corresponding *r*-PAIMAs based on 2-methacrylic diester monomers were unable to form such phases. Thus, the precise substitution and orientation of the isosorbide units in the polymethacrylates seem to be crucial for liquid crystallinity in these materials. This also implies that the degree of liquid crystallinity of the PAIMA materials can be readily controlled. Previous studies have shown that the stereochemistry of isosorbide units in polymer structures can have a large influence on physicochemical properties, e.g., solubility and transition temperatures.[26]

The influence of the dynamics of the order−disorder transition and its influence on the viscosity of **PAIMA16**, **PAIMA18**, and **PAIMA20** was studied by melt rheology in a plate−plate geometry. To verify that the polymers were thermally stable under the measurement conditions, a time sweep was initially performed on **PAIMA18** at 100 °C (slightly above its T_i) for 40 min. If the sample degraded via cross-linking or chain scission reactions, the phase angle (δ) was expected to decrease or increase, respectively, and the shear storage modulus (G') would change. However, in the present case, both δ and G' remained constant over time to indicate high stability in the melt state (see Figure 7). This finding also implied that **PAIMA18** may be melt-processed without degradation.

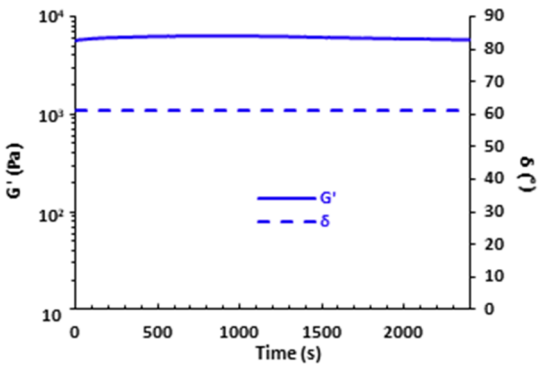

Figure 7. Variation of the melt shear storage modulus (G') and phase shift (δ) during a time sweep of **PAIMA18** at 100 °C, as measured at 1 Hz and 0.01% strain.

In the next step, temperature sweeps were carried out on **PAIMA16**, **PAIMA18**, and **PAIMA20** at 1 Hz in the temperature region around the order−disorder transition. Hence, the samples were first heated to 120 and then cooled to 75 °C at a rate of 2 °C min^{-1}. Next, the polymers were heated to 120 °C before being cooled to 75 °C again at the same rate. Figure 8 shows the complex viscosity as a function of temperature, and the results indicate a stepwise 10−25-fold

https://dx.doi.org/10.1021/acs.biomac.0c01474
Biomacromolecules 2021, 22, 640−648

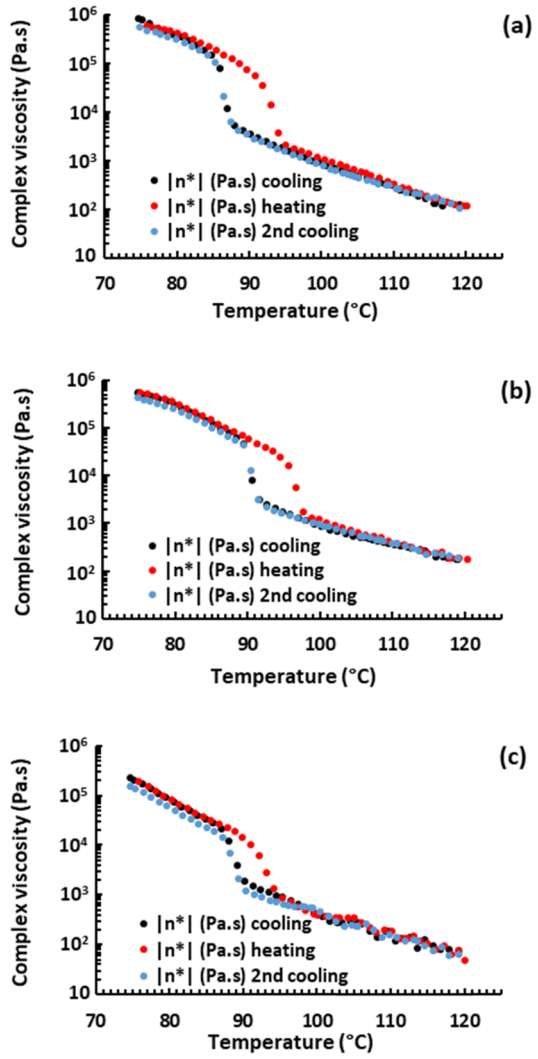

Figure 8. Complex viscosity $|\eta^*|$ of **PAIMA16** (a), **PAIMA18** (b), and **PAIMA20** (c) as a function of temperature (0.01% strain, 1 Hz, 2 °C min^{-1}) showing reversible stepwise changes and hysteresis effects at the order−disorder transitions.

decrease of the complex viscosity at the isotropic transition during heating, followed by a corresponding increase upon subsequent cooling. These steps were reversible and displayed a hysteresis of 4−6 °C. The results thus showed that the viscosity of the liquid crystalline mesophase was higher than that of the isotropic melt phase, most probably because of a higher state of aggregation in the former case.

CONCLUSIONS

We have successfully prepared and systematically explored a series of 12 isosorbide-based AIMA monomers with different pendant linear alkanoyl chains having lengths spanning from C2 to C20. The monomers were synthesized in up to 36 g scale as single regioisomers through biocatalytic and chemical acylation pathways, and were subsequently polymerized by conventional radical polymerization to produce the corresponding series of PAIMA samples. As expected, the alkanoyl chain length had a profound influence on the phase behavior, transition temperatures, and properties of these materials. Hence, PAIMAs tethered with C2−C12 alkanoyl chains were fully amorphous, stiff, and transparent materials with T_g values in the range of 107−66 °C. When the chain length exceeded C13, the polymers in the series became semicrystalline materials with T_m between −4 (C14) and 59 °C (C20). In addition, PAIMAs with C13−C20 chains formed mesophases above T_m and displayed order−disorder transition (ODT) temperatures between 75 (C13) and 94 °C (C20). The appearance of the liquid crystalline mesophases was verified by polarized optical microscopy, and melt rheology showed sharp and reversible changes in the complex viscosity at the ODT during heating−cooling cycles. These measurements also indicated that melt processing is possible without noticeable signs of degradation. Notably, *r*-PAIMA prepared from a regioisomeric C18-monomer showed semicrystallinity but no liquid crystallinity, indicating the crucial role of isosorbide stereochemistry in mesophase formation. The overall study demonstrated that the phase behavior and transition temperatures of the PAIMAs can be controlled by the choice of the alkanoyl chain length and the regiochemistry of the monomer. We envisage that the properties may be further extended and modified using cyclic or branched alkanoyl pendant groups. Hence, the PAIMA class of biobased polymers has the potential to be tailored into viable alternatives in many applications within, e.g., the plastic and coating sectors.

ASSOCIATED CONTENT

Supporting Information

The Supporting Information is available free of charge at https://pubs.acs.org/doi/10.1021/acs.biomac.0c01474.

Detailed descriptions of monomer and polymer synthesis; solubility properties; and SEC chromatograms and NMR spectra (PDF)

AUTHOR INFORMATION

Corresponding Authors

Lauri Vares − *Institute of Technology, University of Tartu, Tartu 50411, Estonia*; Email: lauri.vares@ut.ee

Patric Jannasch − *Institute of Technology, University of Tartu, Tartu 50411, Estonia; Department of Chemistry, Lund University, Lund 221 00, Sweden*; orcid.org/0000-0002-9649-7781; Email: patric.jannasch@chem.lu.se

Authors

Siim Laanesoo − *Institute of Technology, University of Tartu, Tartu 50411, Estonia*

Olivier Bonjour − *Department of Chemistry, Lund University, Lund 221 00, Sweden*

Jaan Parve − *Institute of Technology, University of Tartu, Tartu 50411, Estonia; Department of Chemistry and Biotechnology, Tallinn University of Technology, Tallinn 19086, Estonia*

Omar Parve − *Department of Chemistry and Biotechnology, Tallinn University of Technology, Tallinn 19086, Estonia*

Livia Matt − *Institute of Technology, University of Tartu, Tartu 50411, Estonia*

Complete contact information is available at: https://pubs.acs.org/10.1021/acs.biomac.0c01474

Notes

The authors declare no competing financial interest.

https://dx.doi.org/10.1021/acs.biomac.0c01474
Biomacromolecules 2021, 22, 640−648

■ ACKNOWLEDGMENTS

This work was supported by the European Regional Development Fund and the Estonian Research Council via MOBTT21 and ResTA7 projects, the Estonia-Russia Cross Border Cooperation Program (ER30), and the Baltic Research Program in Estonia (EEA grant no. EMP426). O.B. is grateful to the Swedish Research Council Formas for financial support (diarienr 2016-00468), and P.J. acknowledges funding by the Swedish Foundation for Strategic Environmental Research through the "STEPS" project (No. 2016/1489). O.P. acknowledges the Estonian Research Council (grant PRG339). Sergo Kasvandik and Merilin Saarma are thanked for HRMS analyses, and Rauno Sedrik for graphical abstract.

■ REFERENCES

(1) Sheldon, R. A. The Road to Biorenewables: Carbohydrates to Commodity Chemicals. *ACS Sustainable Chem. Eng.* **2018**, *6*, 4464−4480.
(2) Schneiderman, D. K.; Hillmyer, M. A. 50th Anniversary Perspective: There Is a Great Future in Sustainable Polymers. *Macromolecules* **2017**, *50*, 3733−3749.
(3) Nguyen, H. T. H.; Qi, P.; Rostagno, M.; Feteha, A.; Miller, S. A. The quest for high glass transition temperature bioplastics. *J. Mater. Chem. A* **2018**, *6*, 9298−9331.
(4) Dussenne, C.; Delaunay, T.; Wiatz, V.; Wyart, H.; Suisse, I.; Sauthier, M. Synthesis of isosorbide: an overview of challenging reactions. *Green. Chem.* **2017**, *19*, 5332−5344.
(5) Rose, M.; Palkovits, R. Isosorbide as a Renewable Platform chemical for Versatile Applications—Quo Vadis? *ChemSusChem* **2012**, *5*, 167−176.
(6) Flèche, G.; Huchette, M. Isosorbide. Preparation, Properties and Chemistry. *Starch - Stärke* **1986**, *38*, 26−30.
(7) Saxon, D. J.; Luke, A. M.; Sajjad, H.; Tolman, W. B.; Reineke, T. M. Next-generation polymers: Isosorbide as a renewable alternative. *Prog. Polym. Sci.* **2020**, *101*, No. 101196.
(8) Fenouillot, F.; Rousseau, A.; Colomines, G.; Saint-Loup, R.; Pascault, J. P. Polymers from renewable 1,4:3,6-dianhydrohexitols (isosorbide, isomannide and isoidide): A review. *Prog. Polym. Sci.* **2010**, *35*, 578−622.
(9) Li, Q.; Ma, S.; Wei, J.; Wang, S.; Xu, X.; Huang, K.; Wang, B.; Yuan, W.; Zhu, J. Preparation of Non-Planar-Ring Epoxy Thermosets Combining Ultra-Strong Shape Memory Effects and High Performance. *Macromol. Res.* **2020**, *28*, 480−493.
(10) Cheng, J.; Zhang, P.; Liu, T.; Zhang, J. Preparation and properties of hydrogels based on PEG and isosorbide building blocks with phosphate linkages. *Polymer* **2015**, *78*, 212−218.
(11) Ibert, M.; Buffe, C.; Saint-Loup, R.; Fertier, L.; Robin, J.-J.; Giani, O.; Joly-Duhamel, C. Curable Coating Compositions Containing Unsaturated Dianhydrohexitol Compounds. EP1124909B1, 2014.
(12) Tanaka, H. Easily Peelable Adhesives and Adhesive Film with Good Adhesion.JP20160141142016.
(13) Hong, M.; Tang, X.; Falivene, L.; Caporaso, L.; Cavallo, L.; Chen, E. Y. X. Proton-Transfer Polymerization by N-Heterocyclic Carbenes: Monomer and Catalyst Scopes and Mechanism for Converting Dimethacrylates into Unsaturated Polyesters. *J. Am. Chem. Soc.* **2016**, *138*, 2021−2035.
(14) Kim, S.; Cho, J. K.; Shin, S.; Kim, B.-J. Photo-curing behaviors of bio-based isosorbide dimethacrylate by irradiation of light-emitting diodes and the physical properties of its photo-cured materials. *J. Appl. Polym. Sci.* **2015**, *132*, No. 42726.
(15) Xu, Y.; Hua, G.; Hakkarainen, M.; Odelius, K. Isosorbide as Core Component for Tailoring Biobased Unsaturated Polyester Thermosets for a Wide Structure−Property Window. *Biomacromolecules* **2018**, *19*, 3077−3085.
(16) Stoss, P.; Merrath, P.; Schlüter, G. Regioselektive Acylierung von 1,4:3,6-Dianhydro-D-glucit. *Synthesis* **1987**, *1987*, 174−176.
(17) Gallagher, J. J.; Hillmyer, M. A.; Reineke, T. M. Isosorbide-based Polymethacrylates. *ACS Sustainable Chem. Eng.* **2015**, *3*, 662−667.
(18) Kielty, P.; Smith, D. A.; Cannon, P.; Carty, M. P.; Kennedy, M.; McArdle, P.; Singer, R. J.; Aldabbagh, F. Selective Methylmagnesium Chloride Mediated Acetylations of Isosorbide: A Route to Powerful Nitric Oxide Donor Furoxans. *Org. Lett.* **2018**, *20*, 3025−3029.
(19) Chalecki, Z.; Guibé-Jampel, E. Lipozyme-Mediated Regioselective Esterification of Isosorbide Under Solvent-Free Conditions. *Synth. Commun.* **1997**, *27*, 3847−3852.
(20) Seemayer, R.; Bar, N.; Schneider, M. P. Enzymatic preparation of isomerically pure 1,4:3,6-dianhydro-D-glucitol monoacetates - precursors for isoglucitol 2- and 5-mononitrates. *Tetrahedron: Asymmetry* **1992**, *3*, 1123−1126.
(21) Mukesh, D.; Sheth, D.; Mokashi, A.; Wagh, J.; Tilak, J. M.; Banerji, A. A.; Thakkar, K. R. Lipase catalysed esterification of isosorbide and sorbitol. *Biotechnol. Lett.* **1993**, *15*, 1243−1246.
(22) Brown, C.; Marston, R. W.; Quigley, P. F.; Roberts, S. M. New preparative routes to isosorbide 5-mononitrate. *J. Chem. Soc., Perkin Trans. 1* **2000**, 1809−1810.
(23) Zhu, S.-G.; Huang, J.-X.; Zhang, G.-M.; Chen, S.-X.; Zhang, F.-L. Development of a Practical Enzymatic Synthesis of Isosorbide-2-acetate. *Org. Process Res. Dev.* **2018**, *22*, 1548−1552.
(24) Matt, L.; Parve, J.; Parve, O.; Pehk, T.; Pham, T. H.; Liblikas, I.; Vares, L.; Jannasch, P. Enzymatic Synthesis and Polymerization of Isosorbide-Based Monomethacrylates for High-Tg Plastics. *ACS Sustainable Chem. Eng.* **2018**, *6*, 17382−17390.
(25) Moreno, A.; Bensabeh, N.; Parve, J.; Ronda, J. C.; Cádiz, V.; Galià, M.; Vares, L.; Lligadas, G.; Percec, V. SET-LRP of Bio- and Petroleum-Sourced Methacrylates in Aqueous Alcoholic Mixtures. *Biomacromolecules* **2019**, *20*, 1816−1827.
(26) Beghdadi, S.; Abdelhedi Miladi, I.; Ben Romdhane, H.; Bernard, J.; Drockenmuller, E. RAFT Polymerization of Bio-Based 1-Vinyl-4-dianhydrohexitol-1,2,3-triazole Stereoisomers Obtained via Click Chemistry. *Biomacromolecules* **2012**, *13*, 4138−4145.
(27) Barton, A. *CRC Handbook of Solubility Parameters and Other Cohesion Parameters*; Routledge: New York, 1991.
(28) Thermal Transitions of Homopolymers: Glass Transition & Melting Point. https://www.sigmaaldrich.com/technical-documents/articles/materials-science/polymer-science/thermal-transitions-of-homopolymers.html. (accessed Nov. 25, 2020).
(29) Okouchi, M.; Yamaji, Y.; Yamauchi, K. Contact Angle of Poly(alkyl methacrylate)s and Effects of the Alkyl Group. *Macromolecules* **2006**, *39*, 1156−1159.
(30) Smith, J. C. CXI.—Higher aliphatic compounds. Part I. The systems ethyl palmitate−ethyl stearate and hexa-decyl alcohol−octadecyl alcohol. *J. Chem. Soc.* **1931**, 802−807.
(31) Sasin, G. S.; Schaeffer, P. R.; Sasin, R. Ester Interchange Reactions of Long Chain Thiol Esters1. *J. Org. Chem.* **1957**, *22*, 1183−1184.
(32) PubChem. https://pubchem.ncbi.nlm.nih.gov/compound/Ethyl-arachidate. (accessed Nov. 25, 2020).
(33) He, X.-Z.; Zhang, F.-d.; Jia, Y.; Meng, F.-B.; Jia, Y.-g. Branched-arm macromolecule liquid crystals-containing fluorine and isosorbide-structure and properties. *J. Mol. Struct.* **2015**, *1092*, 96−103.
(34) Zhang, B. Y.; Zheng, Y. Y.; Xu, Y.; Lu, H. W. Synthesis and characterization of side chain cholesteric liquid crystalline polymers containing isosorbide as a chiral centre. *Liq. Cryst.* **2005**, *32*, 357−365.

https://dx.doi.org/10.1021/acs.biomac.0c01474
Biomacromolecules 2021, 22, 640−648